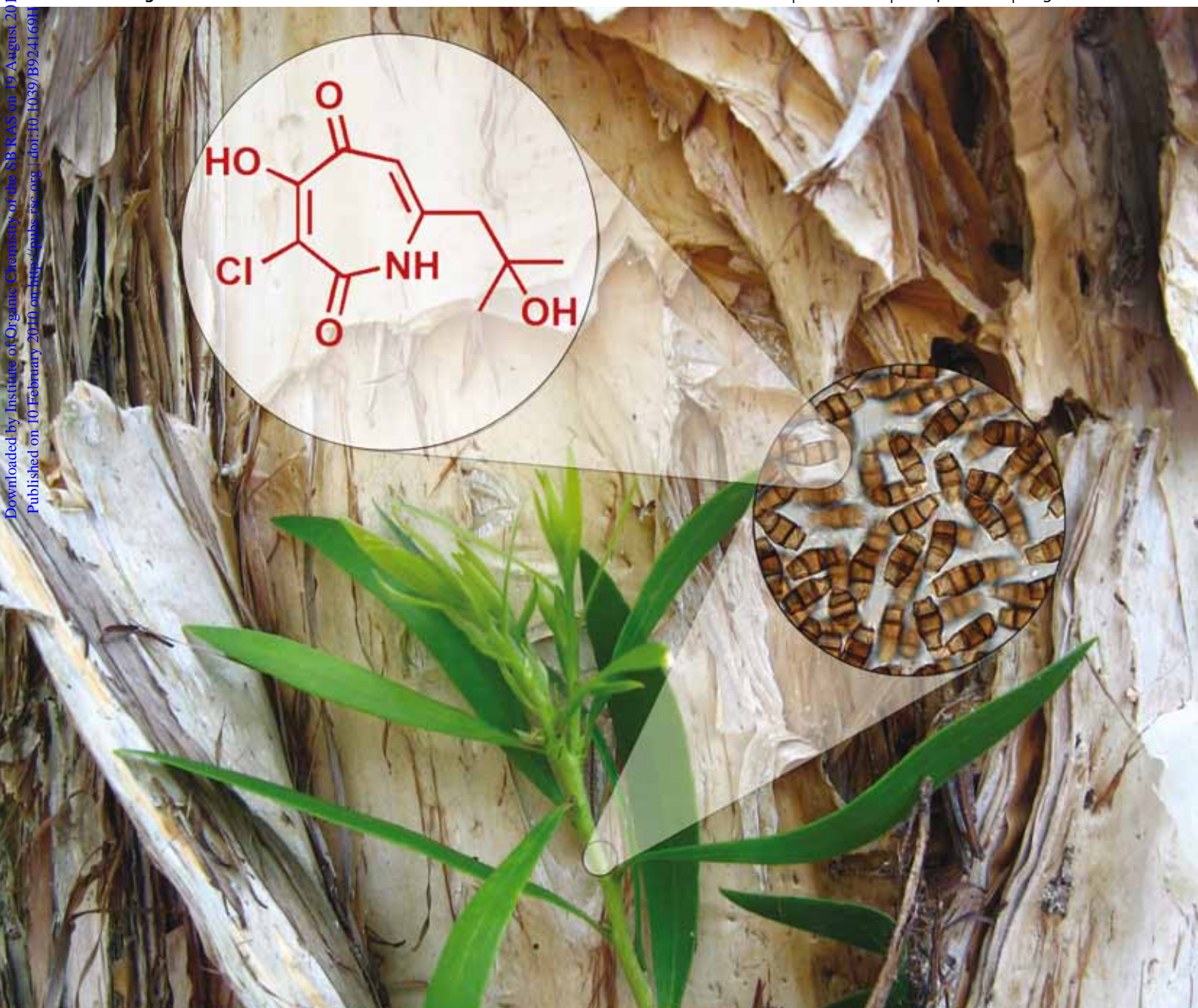


Organic & Biomolecular Chemistry

www.rsc.org/obc

Volume 8 | Number 8 | 21 April 2010 | Pages 1733–1976

Downloaded by Institute of Organic Chemistry of the SB RAS on 10 August 2010
 Published on 10 February 2010 on http://pubs.rsc.org | doi:10.1039/B924169H



ISSN 1477-0520

RSC Publishing

FULL PAPER

Rohan A. Davis *et al.*
 Pestalactams A–C: Novel caprolactams
 from the endophytic fungus
Pestalotiopsis sp.

PERSPECTIVE

Shao Q. Yao *et al.*
 The use of click chemistry in the
 emerging field of catalomics



1477-0520(2010)8:8;1-C

Pestalactams A–C: novel caprolactams from the endophytic fungus *Pestalotiopsis* sp.†

Rohan A. Davis,^{*a} Anthony R. Carroll,^a Katherine T. Andrews,^{a,b} Glen M. Boyle,^b Truc Linh Tran,^b Peter C. Healy,^a John A. Kalaitzis^c and Roger G. Shivas^d

Received 19th November 2009, Accepted 22nd January 2010

First published as an Advance Article on the web 10th February 2010

DOI: 10.1039/b924169h

Chemical investigations of a fermentation culture from the endophytic fungus *Pestalotiopsis* sp. yielded three novel caprolactams, pestalactams A–C (1–3). The structures of 1–3 were determined by analysis of 1D and 2D-NMR, UV, IR, and MS data. The structure of pestalactam A was confirmed following single crystal X-ray diffraction analysis. Pestalactams A–C are the first C-7 alkylated caprolactam natural products to be reported. Pestalactams A (1) and B (2) were tested against two different strains of the malaria parasite *Plasmodium falciparum* (3D7 and Dd2), and the mammalian cell lines, MCF-7 and NFF, and showed modest *in vitro* activity in all assays.

Introduction

Over the decades microfungi have been a source of numerous novel, and bioactive secondary metabolites.^{1,2} Although there has recently been a significant increase in research activity on natural products from marine fungi,^{3–5} terrestrial fungi continue to provide natural products chemists with new and/or biologically interesting compounds. Recent examples of terrestrial-derived fungal compounds include the antileishmanial palmarumycins CP₁₇ and CP₁₈, from the endophyte *Edenia* sp.,⁶ the anticancer berkeleyic acid from *Penicillium* sp.,⁷ farinomalein from *Paecilomyces farinosus*,⁸ the insecticidal paraherquamides H and I from *Penicillium chumiae*,⁹ and the antimalarial polyketide codinaeopsin from the endophytic fungus, *Codinaeopsis gonytrichoides*.¹⁰ As part of our research^{11–15} on the chemistry of endophytic fungi from Australian plants we examined the stems of *Melaleuca quinquenervia* (family Myrtaceae) for its fungal content. Several different microfungi strains were purified and taxonomically identified, including one *Pestalotiopsis* sp. (BRIP 39872). Chemical investigations of static rice fermentation cultures of this endophytic fungal strain yielded three novel caprolactam derivatives, named pestalactams A–C. Herein, the isolation, structure elucidation and preliminary biological evaluations of these novel fungal secondary metabolites are reported.

Results and discussion

The fungus *Pestalotiopsis* sp. was grown on damp white rice under static conditions then extracted with EtOAc. This extract was purified by C₁₈ flash column chromatography using H₂O (0.1% TFA) and increasing amounts of MeOH to yield 11 fractions. Fractions 3–4 were combined and further purified by C₁₈ HPLC [H₂O (0.1% TFA)/MeOH] to yield pestalactams A (1, 19.4 mg) and C (3, 2.0 mg). Fraction 2 from the flash column was purified using C₈ HPLC [H₂O (0.1% TFA)/MeCN] to yield pestalactam B (2, 3.0 mg) (Fig. 1).

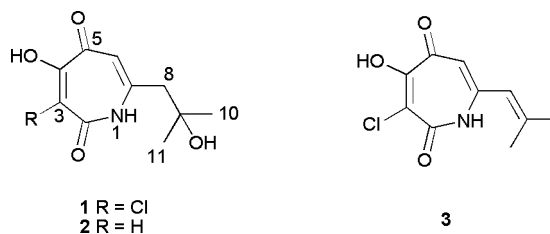


Fig. 1 Chemical structures for pestalactams A–C (1–3).

The major metabolite, pestalactam A (1) was isolated as pale red needles. The (+)-LRESIMS of 1 displayed two pseudomolecular ions at *m/z* 245 and 247 in a relative intensity ratio of 3:1, indicating the molecule contained one chlorine atom. The ¹H and ¹³C NMR data (Table 1) in conjunction with the (+)-HRESIMS allowed a molecular formula of C₁₀H₁₂ClNO₄ to be assigned to 1. The ¹H NMR spectrum displayed only six unique resonances, three of which (δ_H 11.01, 10.94 and 4.98) were determined to be exchangeable following deuterium exchange NMR experiments with D₂O. The remaining protons at δ_H 5.95 (s, 1H), 2.56 (s, 2H) and 1.16 (s, 6H) were attached to carbons resonating at δ_C 108.7, 48.3 and 29.1, respectively, following HSQC data analysis. Nine unique carbons signals, six of which were quaternary, were identified in the ¹³C NMR spectrum of 1. Two downfield carbons (δ_C 174.9 and 160.3) were assigned to carbonyl groups and this was supported by strong absorptions in the IR spectrum at 1674 and 1614 cm⁻¹. A *gem*-dimethyl was established on the basis of a

^aEskitis Institute, Griffith University, Brisbane, QLD 4111, Australia. E-mail: r.davis@griffith.edu.au; Fax: +61-7-3735-6001; Tel: +61-7-3735-6043

^bQueensland Institute for Medical Research, Herston, Queensland, Australia, 4006; Griffith Medical Research College, a joint program of Griffith University and QIMR, Herston, Queensland, Australia

^cSchool of Biotechnology and Biomolecular Sciences, The University of New South Wales, Sydney, NSW 2052, Australia

^dQueensland Primary Industries and Fisheries, Indooroopilly, QLD 4068, Australia

† Electronic supplementary information (ESI) available: ¹H and ¹³C NMR data for pestalactams A–C (1–3), hydrogen bonding network in the crystal structure of pestalactam A (1). CCDC reference number 748402. For ESI and crystallographic data in CIF or other electronic format see DOI: 10.1039/b924169h

strong HMBC correlation between the protons at δ_{H} 1.16 and the carbon (δ_{C} 29.1) to which they were attached (Fig. 2). Furthermore the *gem*-dimethyl system showed other HMBC correlations to carbons, δ_{C} 149.5, 48.3 and 69.8. These data combined with the ROESY correlations between the methyl signal at δ_{H} 1.16 and the methylene unit at δ_{H} 2.56 and the exchangeable proton at δ_{H} 4.98, allowed a 2-methylpropan-2-ol substructure to be assigned. The $^4J_{\text{CH}}$ HMBC correlation from the methyl protons at δ_{H} 1.16 to the carbon at δ_{C} 149.5 suggested that the $(\text{CH}_3)_2\text{COHCH}_2$ - moiety was attached to a sp^2 carbon substituted by a heteroatom. HMBC correlations from the exchangeable proton at δ_{H} 10.94 to δ_{C} 48.3 established that a protonated nitrogen was attached to δ_{C} 149.5.

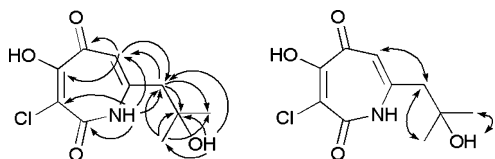


Fig. 2 Key HMBC (\rightarrow) and ROESY (\leftrightarrow) correlations for **1**.

The methine singlet at δ_{H} 5.95 also showed strong HMBC correlations to the methylene carbon (δ_{C} 48.3) and the quaternary methine (δ_{C} 149.5). At this stage it was determined that the remaining portion of **1** consisted of $\text{C}_4\text{O}_3\text{HCl}$. Although no HMBC correlations were identified from the remaining unassigned exchangeable signal at δ_{H} 11.01, the protonated nitrogen resonance at δ_{H} 10.94 showed correlations to δ_{C} 160.3 and 117.0, while the methine singlet at δ_{H} 5.95 showed additional HMBC correlations to δ_{C} 158.4 and 174.9, thus accounting for all carbon atoms in **1**. The weaker HMBC correlations from δ_{H} 5.95 and 10.94 to the carbonyls at δ_{C} 174.9 and 160.3, respectively, suggested that these carbons were only two bonds away from each of these protons. On the basis of a strong HMBC correlation from δ_{H} 5.95 to δ_{C} 158.4, and the fact that the oxygenated exchangeable hydrogen atom (δ_{H} 11.01) remained unassigned, a hydroxyl group was attached to this carbon. The chlorine atom of **1** was attached to the remaining carbon at δ_{C} 117.0. Hence the structure of pestalactam A was assigned to **1**. An X-ray crystal structure of **1** was obtained following refermentation, repurification and crystallization. The ORTEP diagram for **1** is shown in Fig. 3.†

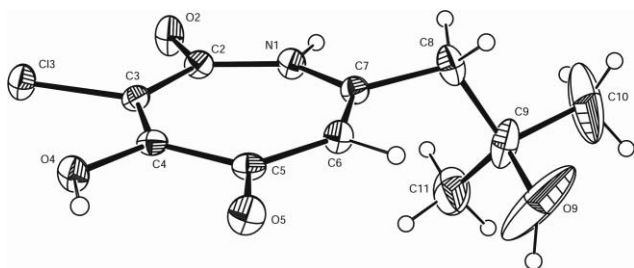


Fig. 3 ORTEP diagram for pestalactam A (**1**). Displacement ellipsoids for non-H atoms are drawn at the 30% level.

† X-Ray crystal data for **1**: $\text{C}_{10}\text{H}_{12}\text{ClNO}_4$, $M = 245.7$, monoclinic, space group $P2_1/a$, $a = 14.466(4)$, $b = 6.563(2)$, $c = 12.390(4)$ Å, $\beta = 111.88(2)^\circ$, $V = 1091.5(6)$ Å³, $Z = 4$, $D_c = 1.49$ g cm⁻³, $\mu = 0.35$ mm⁻¹, Crystal size: $0.55 \times 0.15 \times 0.15$ mm, 2152 reflections collected, 1919 unique ($R_{\text{int}} = 0.037$), $R = 0.063$ [1380 reflections with $I > 2\sigma(I)$], $wR^2 = 0.182$ (all data).

The core seven membered ring, the carbonyl oxygens O2, O5, the hydroxyl oxygen O4, the chloride Cl3 and the methylene carbon C8 are all essentially coplanar with torsion angles ranging from $1.0(7)$ to $-5.9(6)^\circ$. The $(\text{CH}_3)_2\text{COH}$ group lies out of the plane with the C6–C7–C8–C9 torsion angle $79.5(5)^\circ$. The molecules are linked in the crystal lattice through chains of $\text{R}_2^2(9)$ rings along the a glide axis formed by N–H \cdots O and O–H \cdots O hydrogen bonds between the N1–H1 amide and the C5=O5 ketone groups and the O4–H4 hydroxy and C2=O2 carbonyl groups, respectively. The C–C and N–C bond lengths within the seven membered ring are all shorter than the expected values for single bonds with C3–C4 1.357(6), C6–C7 1.353(6) Å shorter than C5–C6 1.425(6), C2–C3 1.462(6) and C4–C5 1.495(5) Å while N1–C2 and N1–C7 are 1.378(5) and 1.370(5) Å, respectively.

Pestalactam B (**2**) was isolated as a pale yellow amorphous solid. The (+)-LRESIMS of **2** displayed a pseudomolecular ion at m/z 212. The 1D-NMR data of **2** were very similar to **1**. The ^{13}C NMR spectra displayed the same number of resonances, the majority of which showed only minor differences in chemical shifts values. The major differences in the two ^{13}C NMR datasets were identified at C-2 ($\Delta = 4.4$ ppm), C-3 ($\Delta = 10.6$ ppm), C-4 ($\Delta = 1.9$ ppm) and C-5 ($\Delta = 2.8$ ppm) of the caprolactam system. The ^1H NMR data readily identified that pestalactam B contained one extra sp^2 proton (δ_{H} 6.13) compared with pestalactam A. These data indicated that **2** was the dechloro derivative of **1**. (+)-HRESIMS and 2D-NMR data analysis confirmed the structure of **2**.

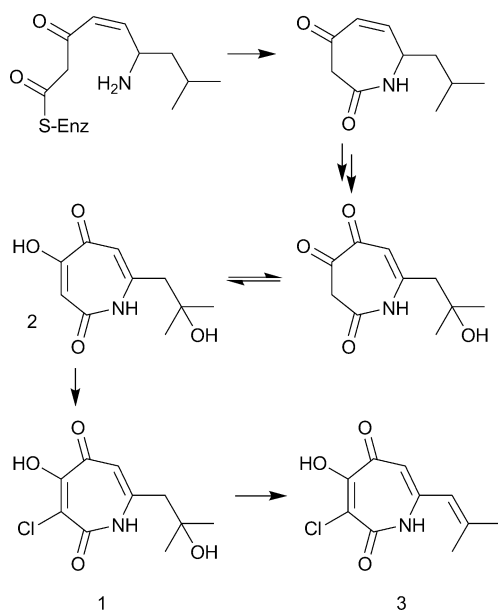
The minor metabolite, pestalactam C (**3**) was purified as a pale-yellow amorphous solid. Analysis of the (+)-LRESIMS indicated the presence of one chlorine atom in **3**, based on the isotopic pattern (3 : 1) of the pseudomolecular ions at m/z 228 and 230. The ^1H and ^{13}C NMR data in conjunction with the (+)-HRESIMS allowed a molecular formula of $\text{C}_{10}\text{H}_{10}\text{ClNO}_3$ to be assigned to **3**. Comparison of the molecular formula of **3** with **1** showed that pestalactam C contained one less oxygen and two less hydrogen atoms, suggesting that **3** was the dehydrated derivative of **1**. Analysis of the ^{13}C NMR spectrum of **3** showed that this compound shared 6 similar carbon resonances (Δ ^{13}C : 0.2–3.3 ppm) with **1**, all of which could be assigned to the same chlorinated caprolactam skeleton present in pestalactam A. Furthermore the upfield carbon signals (δ_{C} 48.3, 69.8 and 29.1) observed in **1** had been replaced with resonances at δ_{C} 121.0, 149.9, 26.5 and 20.1 in **3**. These data coupled with the ^1H NMR spectrum of **3**, which contained an unassigned sp^2 proton singlet at δ_{H} 6.00 (s, 1H) and two methyl singlets at δ_{H} 1.87 (s, 6H), suggested a trisubstituted olefinic moiety was present in **3**. ROESY, HMBC, HSQC data analysis confirmed this moiety and linkage of this olefinic unit to the caprolactam system was established *via* HMBC correlations from δ_{H} 6.01 to δ_{C} 107.5, and from δ_{H} 5.84 to δ_{C} 121.0. Hence, pestalactam C was assigned structure **3**.

The pestalactam carbon skeleton is presumably derived from leucine and two malonyl-CoA derived acetates and assembled by a hybrid NRPS-PKS. The proposed linear enzyme-bound thioester intermediate is likely released from the complex as a result of a thioesterase-catalyzed cyclisation.¹⁶ Oxidation and hydroxylation of the cyclised NRPS-PKS product by cytochrome P450s gives rise to the putative trione intermediate which, on tautomerisation, provides the enol dione **2** (Scheme 1).

The chlorination of **2** to yield the major product **1** is most likely catalyzed by a heme-dependent chloroperoxidase.^{17,18} The

Table 1 ^1H and ^{13}C NMR data for pestalactams A-C (1-3) in $\text{DMSO}-d_6$

Position	Pestalactam A (1)		Pestalactam B (2)		Pestalactam C (3)	
	δ_c^a	δ_H^b (mult, J in Hz, int.)	δ_c^a	δ_H^b (mult, J in Hz, int.)	δ_c^a	δ_H^b (mult, J in Hz, int.)
1		10.94 (brs, 1H)		10.50 (brs, 1H)		11.26 (brs, 1H)
2	160.3		164.7		160.6	
3	117.0		106.4	6.13 (d, 0.8, 1H)	117.2	
4	158.4		160.3		158.1	
4-OH		11.01 (brs, 1H)		10.30 (brs, 1H)		11.00 (brs, 1H)
5	174.9		177.7		175.1	
6	108.7	5.95 (s, 1H)	109.1	5.84 (d, 1.2, 1H)	107.5	5.84 (s, 1H)
7	149.5		150.3		146.2	
8	48.3	2.56 (s, 2H)	48.5	2.52 (s, 2H)	121.0	6.01 (s, 1H)
9	69.8		69.7		149.8	
9-OH		4.98 (brs, 1H)		4.98 (brs, 1H)		
10	29.1	1.16 (s, 3H)	29.1	1.15 (s, 3H)	26.5	1.87 (s, 3H)
11	29.1	1.16 (s, 3H)	29.1	1.15 (s, 3H)	20.1	1.87 (s, 3H)

^a 125 MHz. ^b 500 MHz.**Scheme 1** Proposed biogenesis of pestalactams A-C (1-3).

enol dione has been long established as the preferred substrate for chlorination and such fungal enzymes are considered to be the prototypical examples of heme-dependent haloperoxidases.¹⁹ Subsequent dehydration of the leucine-derived side chain ultimately yields **3**. The assembly of fungal metabolites by hybrid NRPS-PKSs is rare but not unprecedented and several biosynthesis gene clusters have recently been identified including those encoding the biosynthesis of the cytochalasans²⁰ and the aspyridones.²¹ We anticipate that future biosynthetic studies including characterisation of the biosynthesis gene cluster will reveal that the pestalactams are indeed NRPS-PKS derived, and that their assembly represents an alternative pathway to caprolactam formation and one by which the unique C-7 alkylation can be fully explained.

Prior to submitting pestalactams A-C to the open access compound repository at Eskitis,²² and their initial biological evaluation, purity studies were performed using microfluidics liquid chromatography (μPLC).²³ Analysis of the μPLC data and integration of all UV peaks at 254 nm determined that **1** and **2**

had purities of 95% and 94%, respectively, while pestalactam C (**3**) had degraded.

Table 2 shows the *in vitro* activity of compounds **1** and **2** against chloroquine resistant (Dd2) and chloroquine sensitive (3D7) *P. falciparum* malaria parasite lines, and against two mammalian cell types. MCF-7 is a breast adenocarcinoma cancer cell line and NFF (neonatal foreskin fibroblasts) is a “normal” cell type. These cells are routinely used in toxicity studies to determine compound selectivity for parasite or cancer cells. Compounds **1** and **2** displayed similar antimalarial activity, with ~16–41% parasite growth inhibition achieved at 25 μM . The compounds were only modestly selective for malaria parasites *versus* the mammalian cell lines, with both compounds giving ~12–64% inhibition at 100 μM . The compounds displayed ~3-fold selectivity for MCF-7 breast cancer cells *versus* the NFF control cells.

Conclusions

In summary, this paper describes the isolation and structure elucidation of three new caprolactam analogues, pestalactams A–C. Although 55 caprolactam natural products have been reported in the literature to date,²⁴ caprolactams with unsaturation between C-3/C-4 and C-6/C-7 are rare, with only four natural products known to contain this functionality. These include silvaticamide (**4**) from *Aspergillus silvaticus*,²⁵ hygrocin B (**5**) from *Streptomyces hygroscopicus*,²⁶ and ceratamines A (**6**) and B (**7**) from the marine sponge *Pseudoceratina* sp. (Fig. 4).²⁷

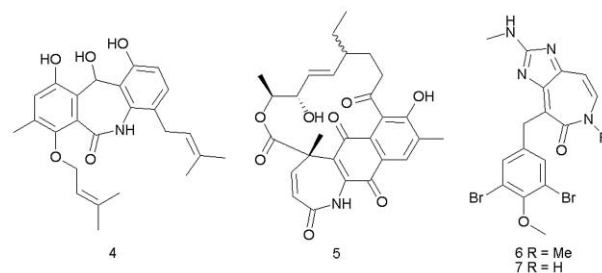
**Fig. 4** Caprolactam natural products 4–7.

Table 2 *In vitro* activity of compounds **1** and **2** against malaria parasites and mammalian cells

Compound	<i>P. falciparum</i> ^a (% inhibition at 25 μM)		Mammalian cells (% inhibition at 100 μM)	
	Dd2	3D7	MCF-7	NFF
1	41.3 (±5.0)	16.2 (±7.6)	64.4 (±3.0)	20.2 (±9.2)
2	36.3 (±3.2)	20.7 (±5.1)	58.5 (±3.2)	12.8 (±4.2)

^a Chloroquine: IC₅₀ 3D7, 0.02 (±0.01) μM; IC₅₀ Dd2, 2.17 (±1.3) μM.

Furthermore, in regards to reported natural product chemistry, compounds **1–3** contain a unique carbon skeleton, due to C-7 alkylation of the caprolactam ring. Pestalactams A and C are the first examples of natural products that contain a halogenated caprolactam ring.

Experimental

General procedures

NMR spectra were recorded at 30 °C on either a Varian 500 MHz or 600 MHz Unity INOVA spectrometer. The latter spectrometer was equipped with a triple resonance cold probe. The ¹H and ¹³C chemical shifts were referenced to the solvent peak for DMSO-*d*₆ at δ_H 2.49 and δ_C 39.5. LRESIMS were recorded on a Waters ZQ mass spectrometer. HRESIMS were recorded on a Bruker Daltonics Apex III 4.7e Fourier-transform mass spectrometer. Melting points were determined using a Gallenkamp digital melting point apparatus and were uncorrected. IR and UV spectra were recorded on a Bruker Tensor 27 spectrometer and a Jasco V650 UV spectrophotometer, respectively. An open glass column (30 mm × 40 mm) packed with Alltech Davisil 30–40 μm 60 Å C₁₈ bonded silica was used for flash chromatography. A Waters 600 pump equipped with a Waters 996 PDA detector and a Waters 717 autosampler were used for HPLC. A Hypersil C₁₈ BDS 5 μm 143 Å column (21.2 mm × 150 mm) and a Hypersil C₈ BDS 5 μm 143 Å column (10 mm × 250 mm) were used for semi-preparative HPLC separations. All solvents used for chromatography, UV, and MS were Lab-Scan HPLC grade, and the H₂O was Millipore Milli-Q PF filtered. All fungal culture media was purchased from Difco.

Collection and identification of fungus

Pestalotiopsis sp. was isolated from a surface sterilised piece of stem (~ 2 mm × 10 mm) from the plant *Melaleuca quinquenervia* collected from Toohey Forest, Queensland, Australia during February of 2003. Sterilisation of the stem fragment was performed by sequential immersion in 95% EtOH (1 min), 2.1% NaOCl (5 min) and 95% EtOH (1 min). The sterilised stem was immediately transferred to a potato dextrose agar (PDA) plate and incubated at 25 °C for 3 days. Developing mycelial colonies were subcultured to fresh PDA plates. Colonies of *Pestalotiopsis* sp. were persistently isolated and one of these cultures was retained (BRIP 39872) for further study. Members of *Pestalotiopsis* are easily recognised by their distinctive conidial morphology, although the determination and delimitation of species in this genus is particularly difficult.²⁸ The identification of *Pestalotiopsis* sp. was based on the presence of acervular conidiomata that produced 4-septate conidia, 22–30 × 6–8 μm, with second, third and fourth cells pale to mid-brown; basal and apical cells hyaline, appendages

on the apical cells mostly 2, unbranched, up to 20 μm long; basal appendage, when present, single, up to 10 μm long. A voucher specimen and living cultures were deposited at the Queensland Primary Industries and Fisheries, Plant Pathology Herbarium, Indooroopilly, QLD 4068, Australia.

Extraction and isolation

The fungal isolate (BRIP 39872) was initially grown on potato dextrose agar, until a prominent growth of mycelia was achieved. The mycelia covered agar was then cut into ~1 cm³ portions, and then transferred to three conical flasks (500 mL) each containing sterilised damp white rice (50 g rice plus 100 mL H₂O). The fermentation was allowed to proceed under static conditions at 25 °C for 28 days after which time the rice and mycelia were extracted with EtOAc (3 × 150 mL). The organic extracts were all combined and the solvent removed *in vacuo* to yield a dark brown gum (3.00 g). This extract was pre-adsorbed to C₁₈ silica (~10 g) overnight then loaded onto a C₁₈ open flash column and a 10% stepwise gradient was performed from H₂O (0.1% TFA) to MeOH; 100 mL washes were used for each eluent step. The 10% MeOH/90% H₂O (0.1% TFA) fraction (40 mg) was further purified by C₈ HPLC using a linear gradient from H₂O (0.1% TFA) to 50% MeCN/50% H₂O (0.1% TFA) in 20 min, followed by another linear gradient to MeCN in 2 min, then isocratic conditions of MeCN for a further 3 min, all at a flow rate of 4 mL min⁻¹. Pestalactam B (**2**, 3.0 mg) was obtained following lyophilisation of the material eluting between 13–13.5 min. The 20% MeOH/80% H₂O (0.1% TFA) and 30% MeOH/70% H₂O (0.1% TFA) eluates from the C₁₈ flash column were combined (81 mg) following ¹H NMR analysis, and subjected to C₁₈ semi-preparative HPLC using a linear gradient from H₂O (0.1% TFA) to MeOH in 50 min, followed by isocratic conditions of MeOH at a flow rate of 6 mL min⁻¹. This afforded pestalactams A (**1**, 19.4 mg) and C (**3**, 2.0 mg), which had retention times of 27–29 and 35–36 min, respectively.

Pestalactam A (1). Pale red needles (MeOH); mp 175–177 °C; UV λ_{max} (MeOH)/nm (log ε) 266 (4.42), 324 (3.76), 360sh (3.51); IR ν_{max}/cm⁻¹ (KBr) 3400–3000, 1674, 1614, 1582, 1494, 1449, 1408, 1339, 1245, 1170, 1130, 1024; ¹H and ¹³C NMR data (DMSO-*d*₆) see Table 1; (+)-LRESIMS *m/z* 246 (100%) [M + H]⁺, 248 (33%) [M + H]⁺; (+)-HRESIMS *m/z* 246.0517 (C₁₀H₁₃³⁵CINO₄ [M + H]⁺ requires 246.0528).

Pestalactam B (2). Pale-yellow amorphous solid; UV λ_{max} (MeOH)/nm (log ε) 263 (4.26), 322 (3.57), 360sh (3.20) nm; IR ν_{max}/cm⁻¹ (KBr) 3400–3100, 1662, 1637, 1602, 1534, 1454, 1410, 1316, 1237, 1199, 1156, 1048; ¹H and ¹³C NMR data (DMSO-*d*₆) see Table 1; (+)-LRESIMS *m/z* 212 (15%) [M + H]⁺, 234 (100%)

[M + Na]⁺; (+)-HRESIMS *m/z* 234.0743 (C₁₀H₁₃NO₄Na [M + Na]⁺ requires 234.0737).

Pestalactam C (3). Pale-yellow amorphous solid; UV (MeOH)/nm (log ϵ) 217 (4.30), 279 (4.41), 327 (4.10), 360 sh (3.95); IR ν_{\max} /cm⁻¹ (KBr) 3400–3100, 1688, 1659, 1407, 1204, 1021; ¹H and ¹³C NMR data (DMSO-*d*₆) see Table 1; (+)-LRESIMS *m/z* 245 (100%) [M + H]⁺, 247 (33%) [M + H]⁺, 250 (100%) [M + Na]⁺, 252 (33%) [M + Na]⁺; (+)-HRESIMS *m/z* 250.0244 (C₁₀H₁₀ClNO₃Na [M + Na]⁺ requires 250.0241).

X-Ray crystallography data for pestalactam A (1)

X-Ray diffraction data for **1** were measured at 295(2) K using a Rigaku AFC7R four circle diffractometer (ω -2 θ) scan mode, graphite monochromated Mo-K α radiation (λ = 0.71069 Å). The structure was solved by direct methods and refined by full matrix least squares refinement on *F*². Anisotropic thermal parameters were refined for non-hydrogen atoms. The peripheral carbon and oxygen atoms of the (CH₃)₂OH group showed high thermal motion reflective of a degree of disorder in this group. The hydrogen atoms bonded to N and C atoms were included at calculated positions and constrained as riding atoms with N–H 0.86 and C–H 0.95 Å. The hydroxyl hydrogen atoms in **1** were located from difference Fourier maps and constrained as riding atoms with O–H 0.85 Å. *U*_{iso}(H) values were set to 1.2 *U*_{eq} on the parent atom. Weights derivative of $w = 1/[\sigma^2(F)]$ were employed. Neutral atom complex scattering factors were employed. Computation used the TeXsan²⁹ and SHELX-97³⁰ program systems and ORTEP-3³¹ and PLATON³² software. CCDC No. 748402.†

P. falciparum growth inhibition assays

In vitro antimalarial growth inhibition assays were carried out using *P. falciparum* lines 3D7 (chloroquine-sensitive) and Dd2 (chloroquine-resistant), as previously described.^{33–35} Briefly, synchronous ring-stage infected erythrocytes (0.5% parasitemia and 2.5% hematocrit) were incubated in triplicate wells of 96-well culture dishes with different concentrations of compound for 48 h before adding 0.5 μ Ci [³H]-hypoxanthine. After incubating for a further 16–24 h, cultures were harvested onto 1450 MicroBeta filter mats (Wallac) and ³H incorporation determined using a 1450 MicroBeta liquid scintillation counter. Percentage inhibition compared to matched DMSO controls (0.5%) was determined and IC₅₀ values calculated using linear interpolation of inhibition curves.³⁶ Three independent experiments were carried out and the mean IC₅₀ (\pm SD) is shown in Table 2.

Mammalian cell assays

All cell lines were cultured in 10% heat-inactivated foetal calf serum (CSL, Australia) in RPMI 1640 medium supplemented with 100 U mL⁻¹ penicillin, 100 μ g mL⁻¹ streptomycin, and 3 mM HEPES at 5% CO₂, 99% humidity at 37 °C. Routine mycoplasma tests were performed using Hoechst stain and were always negative. Cytotoxicities of compounds were determined by clonogenic survival of MCF-7 (breast adenocarcinoma) and human neonatal foreskin fibroblasts (NFF) cells.^{37,38} Cells were plated into 96-well microtitre plates at 5 \times 10³ cells/well, and allowed to adhere overnight. Compounds were added to culture

medium at the indicated final concentrations, and plates incubated in the above conditions for 96 h. Cell survival was then assayed using sulforhodamine B (SRB; Sigma, St. Louis, MO). Briefly, the culture medium was removed from the 96-well microtitre plates and the plates washed twice with phosphate buffered saline (PBS), before the cells were fixed with methylated spirits for 15 min. The plates were then rinsed with tap water and the fixed cells stained with 50 μ L/well of SRB solution (0.4% sulforhodamine B (w/v) in 1% (v/v) acetic acid) over a period of 1 h. The SRB solution was removed from the wells and the plates rapidly washed two times with 1% (v/v) acetic acid. Protein bound dye was then solubilised with the addition of 100 μ L of 10 mM unbuffered Tris, and incubated for 15 min at 25 °C. Plates were then read at 564 nm on a VERSA max tuneable microplate reader (Molecular Devices, Sunnyvale, CA). Data were taken from a minimum of triplicate in at least 2 separate experiments, and expressed as percentage inhibition from cells treated with vehicle alone.

Acknowledgements

The authors thank Bob Coutts (Griffith University) for assistance with the plant identification, and Hoan The Vu (Griffith University) for HRESIMS measurements.

Notes and references

- W. B. Turner, *Fungal Metabolites*, Academic Press, London, New York, 1971.
- W. B. Turner and D. C. Aldridge, *Fungal Metabolites II*, Academic Press, London, New York, 1983.
- A. Piorko, *Fungi*, 2007, 208–235.
- M. Saleem, M. S. Ali, S. Hussain, A. Jabbar, M. Ashraf and Y. S. Lee, *Nat. Prod. Rep.*, 2007, **24**, 1142–1152.
- T. S. Bugni and C. M. Ireland, *Nat. Prod. Rep.*, 2004, **21**, 143–163.
- S. Martinez-Luis, G. Della-Togna, P. D. Coley, T. A. Kursar, W. H. Gerwick and L. Cubilla-Rios, *J. Nat. Prod.*, 2008, **71**, 2011–2014.
- A. A. Stierle, D. B. Stierle and K. Kelly, *J. Org. Chem.*, 2006, **71**, 5357–5360.
- S. P. Putri, H. Kinoshita, F. Ihara, Y. Igarashi and T. Nihira, *J. Nat. Prod.*, 2009, **72**, 1544–1546.
- M. P. Lopez-Gresa, M. C. Gonzalez, L. Ciavatta, I. Ayala, P. Moya and J. Primo, *J. Agric. Food Chem.*, 2006, **54**, 2921–2925.
- R. Kontnik and J. Clardy, *Org. Lett.*, 2008, **10**, 4149–4151.
- R. A. Davis, *J. Nat. Prod.*, 2005, **68**, 769–772.
- R. A. Davis, V. Andjic, M. Kotiw and R. G. Shivas, *Phytochemistry*, 2005, **66**, 2771–2775.
- R. A. Davis, J. Longden, V. M. Avery and P. C. Healy, *Bioorg. Med. Chem. Lett.*, 2008, **18**, 2836–2839.
- R. A. Davis, D. Watters and P. C. Healy, *Tetrahedron Lett.*, 2005, **46**, 919–921.
- P. C. Healy, A. Hocking, N. Tran-Dinh, J. I. Pitt, R. G. Shivas, J. K. Mitchell, M. Kotiw and R. A. Davis, *Phytochemistry*, 2004, **65**, 2373–2378.
- S. A. Sieber and M. A. Marahiel, *Chem. Rev.*, 2005, **105**, 715–738.
- L. P. Hager, D. R. Morris, F. S. Brown and H. Eberwein, *J. Biol. Chem.*, 1966, **241**, 1769–1777.
- D. R. Morris and L. P. Hager, *J. Biol. Chem.*, 1966, **241**, 1763–1768.
- F. H. Vaillancourt, E. Yeh, D. A. Vosburg, S. Garneau-Tsodikova and C. T. Walsh, *Chem. Rev.*, 2006, **106**, 3364–3378.
- J. Schumann and C. Hertweck, *J. Am. Chem. Soc.*, 2007, **129**, 9564–9565.
- S. Bergmann, J. Schumann, K. Scherlach, C. Lange, A. A. Brakhage and C. Hertweck, *Nat. Chem. Biol.*, 2007, **3**, 213–217.
- http://www.griffith.edu.au/science/queensland-compound-library.

- 23 G. K. Pierens, A. R. Carroll, R. A. Davis, M. E. Palframan and R. J. Quinn, *J. Nat. Prod.*, 2008, **71**, 810–813.
- 24 *Dictionary of Natural Products on CD-Rom*, Chapman and Hall/CRC Press, London, UK, 2009, vol. 18.1.
- 25 M. Yamazaki, H. Fujimoto, Y. Ohta, Y. Iitaka and A. Itai, *Heterocycles*, 1981, **15**, 889–893.
- 26 P. Cai, F. Kong, M. E. Ruppen, G. Glasier and G. T. Carter, *J. Nat. Prod.*, 2005, **68**, 1736–1742.
- 27 E. Manzo, R. van Soest, L. Matainaho, M. Roberge and R. J. Andersen, *Org. Lett.*, 2003, **5**, 4591–4594.
- 28 R. Jeewon, E. C. Liew, J. A. Simpson, I. J. Hodgkiss and K. D. Hyde, *Mol. Phylogenet. Evol.*, 2003, **27**, 372–383.
- 29 *TeXsan for Windows, Version 1.06*. MSC 9009 New Trails Drive, The Woodlands, TX 77381, USA, 1997–2001.
- 30 G. M. Sheldrick, *Acta Crystallogr. A*, 2008, **64**, 112–122.
- 31 L. J. Farrugia, *J. Appl. Crystallogr.*, 1997, **30**, 565.
- 32 A. L. Spek, *Acta Crystallogr., Sect. D: Biol. Crystallogr.*, 2009, **65**, 148–155.
- 33 K. T. Andrews, T. N. Tran, A. J. Lucke, P. Kahnberg, G. T. Le, G. M. Boyle, D. L. Gardiner, T. S. Skinner-Adams and D. P. Fairlie, *Antimicrob. Agents Chemother.*, 2008, **52**, 1454–1461.
- 34 G. S. Dow, Y. Chen, K. T. Andrews, D. Caridha, L. Gerena, M. Gettayacamin, J. Johnson, Q. Li, V. Melendez, N. Obaldia 3rd, T. N. Tran and A. P. Kozikowski, *Antimicrob. Agents Chemother.*, 2008, **52**, 3467–3477.
- 35 D. Walliker, I. A. Quakyi, T. E. Wellems, T. F. McCutchan, A. Szarfman, W. T. London, L. M. Corcoran, T. R. Burkot and R. Carter, *Science*, 1987, **236**, 1661–1666.
- 36 W. Huber and J. C. Koella, *Acta Trop.*, 1993, **55**, 257–261.
- 37 S. M. Ogbourne, A. Suhrbier, B. Jones, S. J. Cozzi, G. M. Boyle, M. Morris, D. McAlpine, J. Johns, T. M. Scott, K. P. Sutherland, J. M. Gardner, T. T. Le, A. Lenarczyk, J. H. Aylward and P. G. Parsons, *Cancer Res.*, 2004, **64**, 2833–2839.
- 38 S. J. Cozzi, P. G. Parsons, S. M. Ogbourne, J. Pedley and G. M. Boyle, *Cancer Res.*, 2006, **66**, 10083–10091.